

## TWO-DIMENSIONAL EXPERIMENTAL ELASTIC-PLASTIC STRAIN AND STRESS ANALYSIS

BARBARA KOZŁOWSKA

*Warsaw University of Technology, Faculty of Mechatronic Engineering, Warsaw, Poland*

*e-mail: b.kozłowska@mchtr.pw.edu.pl*

In the paper, the quantitative analysis of elastic-plastic state of strain and stress in two-dimensional models with different stress concentrators is presented. The experimental testing was carried out by the photoelastic coating method on duralumin elements loaded by tensile stresses. For strain separation, the analytical method of characteristics, taking advantage of an isochromatic pattern only, was applied. The strain and stress components in elastic-plastic areas around stress concentrators were calculated using the multi-sectional schematization of the material curve. The effects of investigations have been compared with those obtained from Moiré method and numerical calculation (FEM). The discussion of results has been presented.

*Key words:* mechanics of solids, experimental methods, elastic-plastic states

### 1. Introduction

Exploitation conditions of many constructions often create partial material plastifying. Considering the safety of the whole structure, the knowledge about the process of deformation after crossing the yield point is very important.

The simulation of non-linear problems, like the modelling of a structural material – the character of strain hardening or conversion from elastic to plastic state, may cause many difficulties as well as the modelling of real object itself (shape, loading conditions, etc.).

The widely applied nowadays numerical methods (FEM, e.g) always contain some inaccuracy and their results should be verified experimentally.

Experimental elastic-plastic states investigations are conducted in many research centers all over the world, and a great variety of problems is considered like: estimation of the bearing capacity of constructional elements and the localization of places, where plastic pseudo-joints can be created (Livieri and Nicoletto, 2003; Milke *et al.*, 2000; Padmanabhan *et al.*, 2006); the analysis of residual stress caused by material plastifying (e.g in the process of machining) (Gurova *et al.*, 1998; Kelleher *et al.*, 2003; Rasty *et al.*, 2007); estimation of residual (plastic) strain remaining in the material after removing loading (Diaz *et al.*, 2004; Haldrup *et al.*, 2008) and the investigation of large (plastic) deformation (Fontanari *et al.*, 2006; Franck *et al.*, 2007; Tong, 2004).

Apart from these specific problems of elastic-plastic states investigation, the general case of quantitative strain and stress analysis in the plastified zones is of great importance. It concerns any object working in the over-elastic range and makes possible to estimate how the partial plastifying of the element affect the state of the total structure.

In such cases, experimental methods, which allow analyzing real constructions under working conditions, seem to be very useful.

One of the experimental methods, which can be applied to elastic-plastic states analysis, is the photoelastic coating method. The method gives information about deformation of the whole tested area (not only at several points). It can be used to investigate objects of different sizes

and shapes, loaded in different ways (dynamically and statically) also in the over-elastic range and at various temperatures ( $-20^{\circ}\text{C}$ - $50^{\circ}\text{C}$ ).

## 2. Photoelastic coating method in elastic-plastic states analysis

The photoelastic coating method makes use of the effect of optical birefringence which occurs in some transparent materials under loading (Zandman *et al.*, 1977). It is based on the assumption that there is a univocal dependence between the strain occurring on the surface of an analyzed element and the deformation of the thin layer of the birefringent material integrally bonded to this surface. When the object is loaded, the surface strains are transmitted to the coating, which may be observed through a reflection polariscope. In that case, the loaded coating exhibits two families of fringe patterns:

- isoclinic fringes – lines, along which the directions of the principal strains are constant

$$\alpha_n = \text{const} \quad (2.1)$$

where  $\alpha_n$  is the angle between the direction of the greater principal strain component and the accepted reference direction  $x$ ;

- isochromatic fringes – lines, along which the difference of the principal strains is constant

$$\varepsilon_1 - \varepsilon_2 = N f_\varepsilon \quad (2.2)$$

where:  $\varepsilon_1$ ,  $\varepsilon_2$  – principal strain components,  $N$  – value of the isochromatic order,  $f_\varepsilon$  – strain constant of the photoelastic coating.

Obtained from the photoelastic coating method information is not sufficient for determining all strain components in the general case of two-dimensional state of stress occurring on the surface of the analyzed object. Besides, the measurement of the isoclinic parameter is labour-consuming and usually not precise. Therefore, to the principal strain separation one may use additional information obtained from other experimental methods or analytical (or numerical) methods.

The method of photoelastic coating can be applied to strain analysis in partly plastified elements. This possibility results from the linear relation between the photoelastic effect and strain in the birefringent material in a wide range. The characteristics of most epoxy resins used as photoelastic coatings are linear in the range of strains, where the tested material is already plastified.

One of the methods, which enable the experimental data analysis, is the method of characteristics (Szczepiński, 1964). It allows determining strain components, in a relatively simple way, using the isochromatic pattern only.

The method of characteristics was originally proposed for the elastic states analysis, because for strain separation the relations between the strain and stress components (Hooke's law) as well as the equations of equilibrium and the strain compatibility condition are used (Kapkowski *et al.*, 1987).

The application of the method to strain separation in plastified zones required formulating relations between the strain and stress components (for the two-dimensional state of stress) in the non-linear part of  $\sigma(\varepsilon)$  curve (Kapkowski and Kozłowska, 1993; Kozłowska, 1996).

These relations were derived on the basis of the accepted geometrical model of the material characteristic, where the experimentally obtained curve is replaced by  $n$  line segments (Fig. 1a). Each of these segments describes a different state of the material and is characterized by a different modulus of elasticity  $E_i$  and the Poisson ratio  $\nu_i$ . The points  $K_i$  define the change of

the material state and each time they are matched for the constructional material on the basis of the real  $\sigma(\varepsilon)$  curve. They determine the change of the slope angle of straight segments of the material characteristic ( $i = 1$  refers to the elastic state and  $i = 2, \dots, n - 1$  stands for the successive over-elastic states). These points correspond to the stresses  $\sigma_{(K)_i}$ .

Deriving relationships between the strain and stress components in the over-elastic range for a two-dimensional state of stress using the multi-sectional model requires making assumptions referring to the course of the deformation process after crossing the yield point (Kapkowski and Kozłowska, 1993; Kozłowska, 1996). They are as follows:

- The relationship  $\sigma(\varepsilon)$  has the same character (the same values of the modulus of elasticity and the Poisson ratio) for both principal directions as under the uniaxial tension. It means that successive segments of the characteristics:  $\sigma(\varepsilon)$ ,  $\sigma_1(\varepsilon_1)$ ,  $\sigma_2(\varepsilon_2)$  are parallel (Fig. 1b). Where:  $(K_1)_i$ ,  $(K_2)_i$  – points analogous to the points  $(K)_i$  (points of the change of the slope angle of straight segments of the material characteristic – Fig. 1a) for both principal directions of the two-dimensional state of stress.
- The strain hardening of the material has the isotropic character and the change of state of the material takes place at the constant ratio  $\sigma_2/\sigma_1$ .

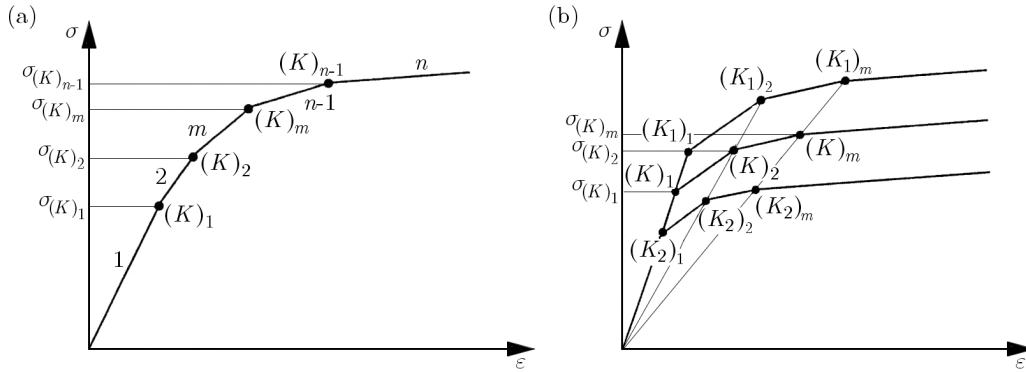


Fig. 1. Multi-sectional model of the material characteristic: (a) for uniaxial tension, (b) for two-dimensional state of stress

The principal stresses characterizing material conversion from the elastic state to the first over-elastic state and from one over-elastic state to every next one can be described as

$$(\sigma_1)_{(K_1)_i} = (k_1)_i \sigma_{(K)_i} \quad (\sigma_2)_{(K_2)_i} = (k_2)_i \sigma_{(K)_i} \quad (2.3)$$

where:  $(\sigma_1)_{(K_1)_i}$ ,  $(\sigma_2)_{(K_2)_i}$  – stresses corresponding to the points of the change of the slope angle of straight segments of the material characteristic for both principal directions of two-dimensional state of stress ( $i = 1, \dots, n - 1$ );  $(k_1)_i$ ,  $(k_2)_i$  – coefficients characterizing stress components at the moment of material state change in both principal directions.

The assumptions enable univocal determination of the multi-sectional schematization of the  $\sigma(\varepsilon)$  relationship for the two-dimensional state of stress. If the principal stress components in the points  $(K_1)_i$ ,  $(K_2)_i$  are described by formulas (2.3), the coefficients  $(k_1)_i$ ,  $(k_2)_i$  satisfy the relationships

$$\begin{aligned} (k_1)_1 &= (k_1)_2 = \dots = (k_1)_i = \dots = (k_1)_{n-1} = k_1 \\ (k_2)_1 &= (k_2)_2 = \dots = (k_2)_i = \dots = (k_2)_{n-1} = k_2 \end{aligned} \quad (2.4)$$

Defining of multi-sectional model of the material characteristic for two-dimensional state of stress enables one to formulate relationships between the principal strain and stress components at any over-elastic stage

$$\begin{aligned}
(\varepsilon_1)_m &= \frac{1}{E_m} [(\sigma_1)_m - \nu_m(\sigma_2)_m] + \sum_{i=2}^m \sigma_{(K)_{i-1}} \left[ \frac{1}{E_{i-1}} (k_1 - \nu_{i-1}k_2) - \frac{1}{E_i} (k_1 - \nu_i k_2) \right] \\
(\varepsilon_2)_m &= \frac{1}{E_m} [(\sigma_2)_m - \nu_m(\sigma_1)_m] + \sum_{i=2}^m \sigma_{(K)_{i-1}} \left[ \frac{1}{E_{i-1}} (k_2 - \nu_{i-1}k_1) - \frac{1}{E_i} (k_2 - \nu_i k_1) \right]
\end{aligned} \tag{2.5}$$

where:  $(\varepsilon_1)_m, (\varepsilon_2)_m$  – principal strain components at the  $m$ -th stage of over-elastic state of the material;  $(\sigma_1)_m, (\sigma_2)_m$  – principal stress components at the  $m$ -th stage of over-elastic state of the material;  $\nu_m$  – Poisson's ratio at the  $m$ -th stage of over-elastic state of the material;  $E_m$  – modulus of elasticity at the  $m$ -th stage of over-elastic state of the material;  $\nu_i, E_i$  – modulus of elasticity and Poisson's ratio corresponding to succeeding segments of the material characteristic ( $i = 2, \dots, m$ );  $k_1, k_2$  – plastification coefficients in both principal directions.

The plastification coefficients  $k_1, k_2$  characterize the state of stress in every point of the element at moment of appearing first over-elastic strains. From these assumptions, for the multi-sectional model of the material characteristic it results that in these points there must be fulfilled the yield criterion, because the material is not elastic any longer. Taking into account a more general Huber-Mises yield criterion and accepting the stress  $\sigma_{(K)_1}$  (Fig. 1a) for the yield point, we have

$$k_1^2 - k_1 k_2 + k_2^2 = 1 \tag{2.6}$$

where relationship (2.3) for  $i = 1$  was used.

Introducing a more general coefficient (plastification coefficient of the material)

$$k_{pl} = \frac{k_1 - k_2}{2} \tag{2.7}$$

the coefficients  $k_1$  and  $k_2$  can be described as

$$k_1 = \sqrt{1 - 3k_{pl}^2} + k_{pl} \quad k_2 = \sqrt{1 - 3k_{pl}^2} - k_{pl} \tag{2.8}$$

To analyze the results obtained by the photoelastic coating method, it is more convenient to use the sum and the difference of the principal strain and stress components

$$\begin{aligned}
(\varepsilon_1 - \varepsilon_2)_m &= (1 + \nu_m) \left[ \frac{1}{E_m} (\sigma_1 - \sigma_2)_m + 2k_{pl}(w_R)_m \right] \\
(\varepsilon_1 + \varepsilon_2)_m &= (1 - \nu_m) \left[ \frac{1}{E_m} (\sigma_1 + \sigma_2)_m + 2\sqrt{1 - 3k_{pl}^2}(w_S)_m \right]
\end{aligned} \tag{2.9}$$

where the following designations were introduced

$$\begin{aligned}
(w_R)_m &= \frac{1}{1 + \nu_m} \sum_{i=2}^m \sigma_{(K)_{i-1}} \left( \frac{1 + \nu_{i-1}}{E_{i-1}} - \frac{1 + \nu_i}{E_i} \right) \\
(w_S)_m &= \frac{1}{1 - \nu_m} \sum_{i=2}^m \sigma_{(K)_{i-1}} \left( \frac{1 - \nu_{i-1}}{E_{i-1}} - \frac{1 - \nu_i}{E_i} \right)
\end{aligned} \tag{2.10}$$

The equations of equilibrium for the two-dimensional state of stress described in the principal system can be presented in the form

$$\begin{aligned}
\frac{\partial s}{\partial x} + \frac{\partial r}{\partial x} \cos 2\alpha_n + \frac{\partial r}{\partial y} \sin 2\alpha_n + 2r \left( \frac{\partial \alpha_n}{\partial y} \cos 2\alpha_n - \frac{\partial \alpha_n}{\partial x} \sin 2\alpha_n \right) &= 0 \\
\frac{\partial s}{\partial y} + \frac{\partial r}{\partial x} \sin 2\alpha_n - \frac{\partial r}{\partial y} \cos 2\alpha_n + 2r \left( \frac{\partial \alpha_n}{\partial y} \sin 2\alpha_n + \frac{\partial \alpha_n}{\partial x} \cos 2\alpha_n \right) &= 0
\end{aligned} \tag{2.11}$$

where designations:  $s = (\sigma_1 + \sigma_2)/2$  and  $r = (\sigma_1 - \sigma_2)/2$  were introduced.

Using the strain compatibility condition for the two-dimensional state of stress (Timoshenko and Goodier, 1962), relationships (2.9) and dependence (2.2) for the photoelastic coating, equations (2.11) can be presented in a form which is more convenient for the analysis using data obtained from the photoelastic coating method. The difference of principal strain (described by the values of isochromatic order  $N$ ) is the known value, while the searched values are: the sum of principal strain and the angle between the direction of the greater principal strain component and the accepted reference direction  $x$

$$\begin{aligned} & \frac{1}{1-\nu_m} \frac{\partial}{\partial x} \left( \frac{e}{f_\varepsilon} \right) - 2\bar{N} \sin 2\alpha_n \frac{\partial \alpha_n}{\partial x} + 2\bar{N} \cos \alpha_n \frac{\partial \alpha_n}{\partial y} \\ & = (w_S)_m \frac{\partial}{\partial x} \left( 2\sqrt{1-3k_{pl}^2} \right) - \left( \frac{\partial \bar{N}}{\partial x} \cos 2\alpha_n + \frac{\partial \bar{N}}{\partial y} \sin 2\alpha_n \right) \\ & \frac{1}{1-\nu_m} \frac{\partial}{\partial y} \left( \frac{e}{f_\varepsilon} \right) + 2\bar{N} \cos 2\alpha_n \frac{\partial \alpha_n}{\partial x} + 2\bar{N} \sin \alpha_n \frac{\partial \alpha_n}{\partial y} \\ & = (w_S)_m \frac{\partial}{\partial y} \left( 2\sqrt{1-3k_{pl}^2} \right) - \left( \frac{\partial \bar{N}}{\partial x} \sin 2\alpha_n - \frac{\partial \bar{N}}{\partial y} \cos 2\alpha_n \right) \end{aligned} \quad (2.12)$$

where

$$e = \frac{\varepsilon_1 + \varepsilon_2}{2}$$

and  $f_\varepsilon$  – strain constant of the photoelastic coating;  $\alpha_n$  – angle between the direction of the greater principal strain component and the accepted reference direction  $x$ .

To simplify the form of equations (2.12), a new variable  $\bar{N}$  was introduced, whose value may be determined on the basis of distribution of the isochromatic pattern  $N(x, y)$

$$\bar{N} = \frac{N}{2(1+\nu_m)} - (w_R)_m 2k_{pl} \quad (2.13)$$

The obtained system of equations, quasi-linear in relation to derivatives of the unknown functions:  $e/f_\varepsilon$  and  $\alpha_n$ , is always of a hyperbolic type and has two families of real characteristics described by differential equations:

— first family

$$\begin{aligned} & \frac{dy}{dx} = \tan \left( \alpha_n + \frac{\pi}{4} \right) \\ & \frac{1}{2(1-\nu_m)} d \left( \frac{e}{f_\varepsilon} \right) + \bar{N} d(\alpha_n) = \frac{1}{2} (w_S)_m d \left( 2\sqrt{1-3k_{pl}^2} \right) + \frac{1}{2} \left( \frac{\partial \bar{N}}{\partial y} dx - \frac{\partial \bar{N}}{\partial x} dy \right) \end{aligned} \quad (2.14)$$

— second family

$$\begin{aligned} & \frac{dy}{dx} = \tan \left( \alpha_n - \frac{\pi}{4} \right) \\ & \frac{1}{2(1-\nu_m)} d \left( \frac{e}{f_\varepsilon} \right) - \bar{N} d(\alpha_n) = \frac{1}{2} (w_S)_m d \left( 2\sqrt{1-3k_{pl}^2} \right) + \frac{1}{2} \left( \frac{\partial \bar{N}}{\partial x} dy - \frac{\partial \bar{N}}{\partial y} dx \right) \end{aligned} \quad (2.15)$$

These equations allow calculating the values of  $e/f_\varepsilon$  and  $\alpha_n$  by numerical integration over the characteristic curves with the appropriate boundary conditions (Kapkowski and Kozłowska, 1993; Kozłowska, 1996). They supply information necessary for strain separation in the analyzed elastic-plastic zone and full determination of the state of strain.

The relationships between stress and strain components found for the nonlinear part of materials characteristic (2.5) may also be used for calculating stress components in plastified zones of the analyzed elements as well as for strain separation.

### 3. Experimental testing

The investigation of elastic-plastic states by the photoelastic coating method was performed on two-dimensional models weakened by different stress concentrators (holes) and subjected to tensile stresses – Fig. 2. This type of elements and loadings occurs frequently in structural components (Pastrama *et al.*, 2005; Wung *et al.*, 2001) and because of technological or constructional cut-outs needs special attention.

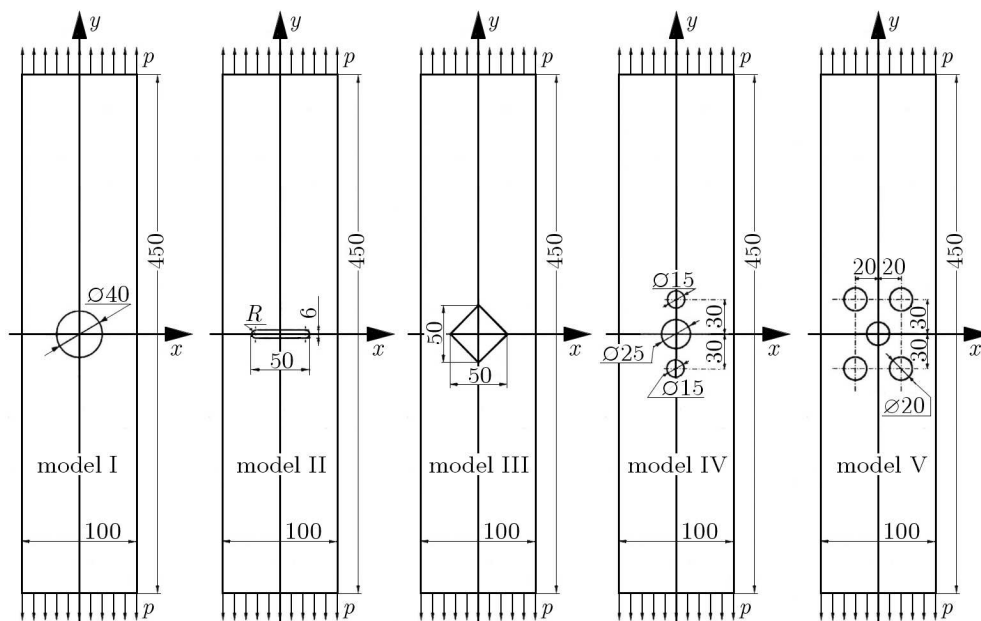


Fig. 2. Models of constructional elements

The models were made of a duralumin sheet 3 mm thick, from which stripes of 100 mm in width and 450 mm in length were cut out. The length of the stripes was taken large enough to compensate potential non-uniformity of tensile stresses distribution applied at their ends.

The characteristic of the material (alloy EN-AW-2024) was determined experimentally on the basis of a standard static uniaxial tensile test (according to PN-EN 10002-1 for tests at ambient temperature). It is shown in Fig. 3.

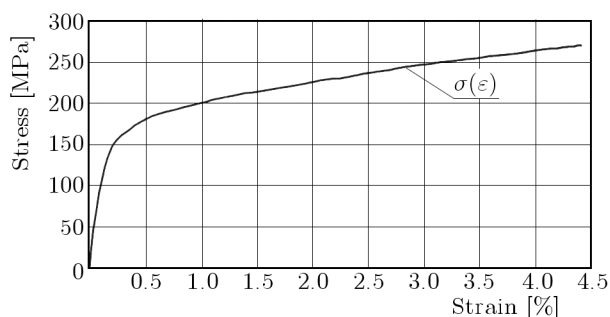


Fig. 3. Material characteristic

After mechanical working and special surface preparation (grinding and etching), the models were covered on both sides (to avoid bending effect) with the photoelastic coating made of epoxy resin. The strain constant of the photoelastic coating:  $f_{\epsilon} = 1.114 \cdot 10^{-3}$  1/fringe order, was determined experimentally. Next, different holes were cut out in the way which allowed avoiding creation of plastic strains as a result of machining. Shapes of the stress concentrators

were designed on the basis of engineering practice (single central holes of various shapes and groups of circular holes of various configurations) – Fig. 2.

The models were loaded at their ends with uniformly distributed tensile stresses ( $p$ ). As the measure of the loading intensity, the ‘loading factor’ ( $s$ ) was accepted. It was calculated as a ratio of the average tensile stresses at the cross-section weakened by the hole on the axis of symmetry perpendicular to the stretching direction in relation to the offset yield strength  $R_{0.2} = 182 \text{ MPa}$  (taken from the material characteristic).

The loading of the models was increased step by step within the over-elastic range of the material. At selected levels of loading, the photographs of the isochromatic pattern were taken twice: for both dark- and light-field polariscope. The stand for testing models is shown in Fig. 4

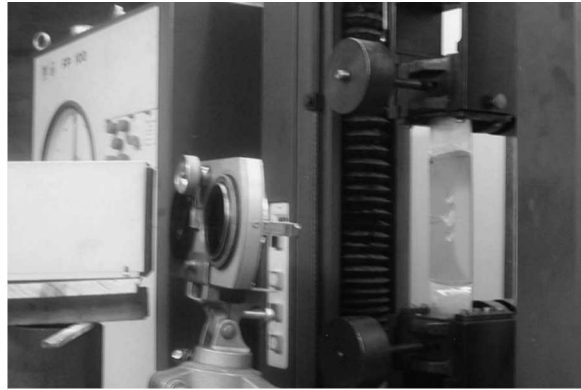


Fig. 4. The stand for testing models by photoelastic coating method

#### 4. Strain and stress analysis in elastic-plastic zones

The results of quantitative analysis of the elastic-plastic strain and stress in the neighborhood of different stress concentrators are presented exemplarily for the model IV (with three circular holes).

The strain separation in the analyzed area was carried out by means of the general field method of characteristics (equations (2.14) and (2.15)) using the 6-sectional geometrical approximation for the  $\sigma$ - $\varepsilon$  curve (Fig. 5).

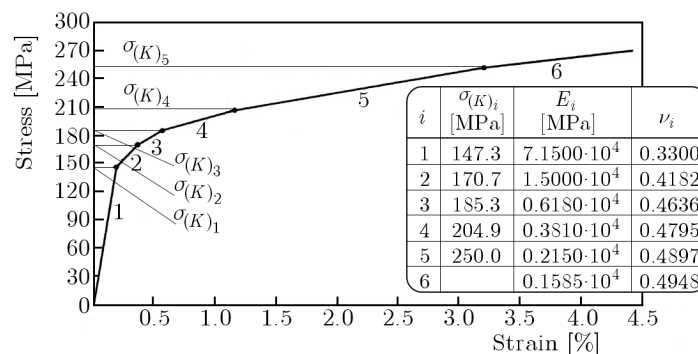


Fig. 5. 6-sectional model of the material characteristic

The isochromatic pattern taken from the dark-field polariscope at the loading level  $s = 0.928$ , which corresponds to tensile stresses  $p = 127 \text{ MPa}$ , is shown in Fig. 6. Because of the symmetry of the model and loading, only one quarter of the tested area has been considered.

On the basis of the isochromatic pattern obtained from this picture, the strain and stress components in the nodes of characteristics were determined. Calculations were started from the non-loaded edge of the central hole (A-B) – (Fig. 6). For determining the isochromatic order in the design point (on the basis of the sinusoidal distribution of the light intensity level), strain separation and stress calculation, a special computer program was used.

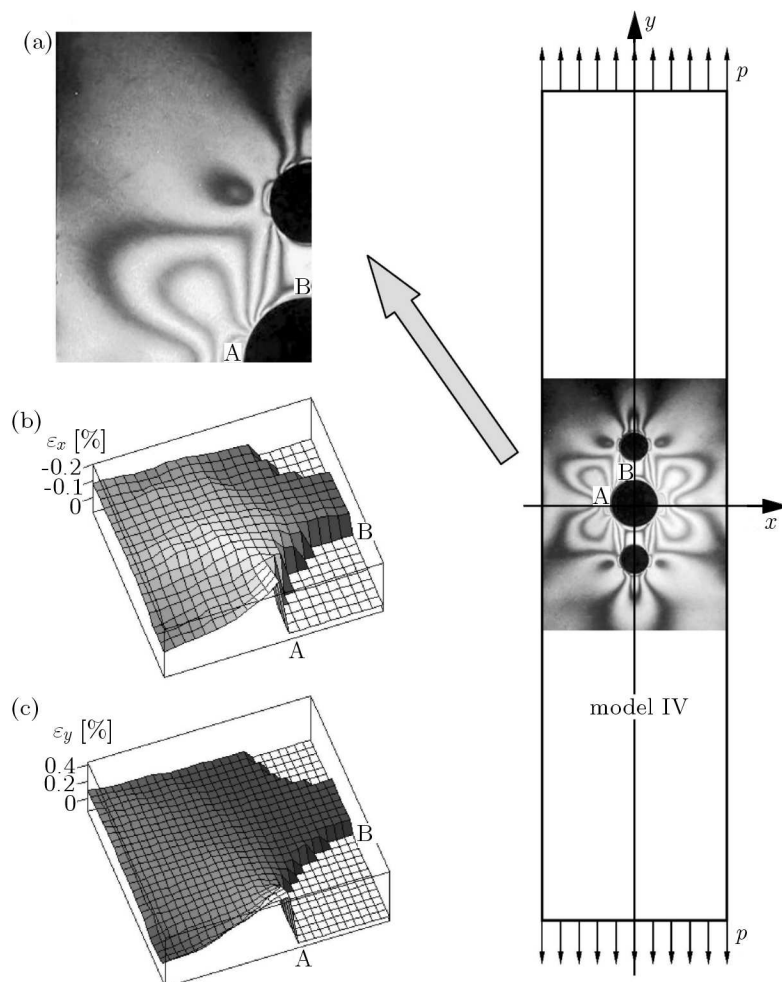


Fig. 6. Analyzed area of model IV at the loading level –  $s = 0.928$ : isochromatic pattern (a), strain  $\varepsilon_x$  distribution (b), strain  $\varepsilon_y$  distribution (c)

For better visualization of the determined strain and stress distributions, the values calculated in the nodes of characteristics (irregular co-ordinates) were recalculated for the nodes of a rectangular grid and graphically represented in form of a surface.

The distribution of strain values  $\varepsilon_x$  and  $\varepsilon_y$  in the analyzed area of model IV are shown in Fig. 6b and Fig. 6c. For better legibility of the diagrams, the values of  $\varepsilon_x(x, y)$  are shown as positive – in reality, they are negative. Extreme values of the calculated strains are:  $\varepsilon_x = -0.297\%$  and  $\varepsilon_y = 0.534\%$ . Figure 7 shows the surfaces representing the stress components  $\sigma_x(x, y)$  and  $\sigma_y(x, y)$ , whose extreme values are:  $\sigma_x = 138$  MPa and  $\sigma_y = 218$  MPa. Because of very small non-dilatational strain and shear stress, the distributions of their values are not presented.

In Fig. 8, the distribution of reduced stress (according to Huber-Mises hypothesis) is presented as well as the range of the over-elastic area determined on the basis of this distribution. It corresponds to the first yield point on the schematization of the material characteristic (Fig. 5).



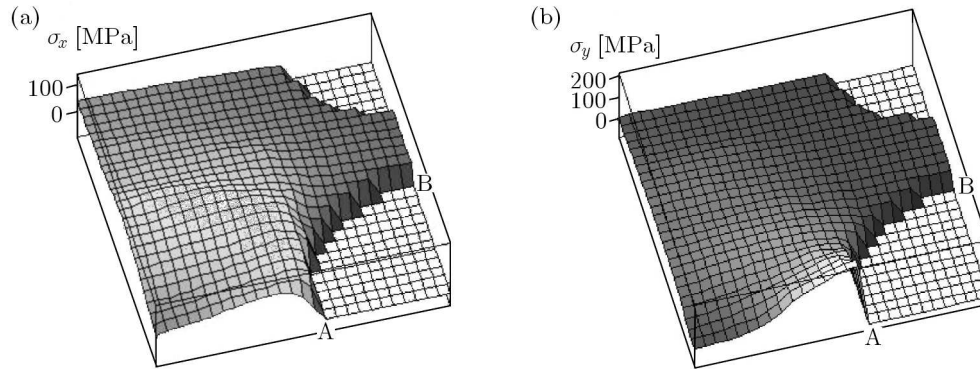


Fig. 7. Analyzed area of model IV at the loading level –  $s = 0.928$ : (a) stress  $\sigma_x$  distribution, (b) stress  $\sigma_y$  distribution

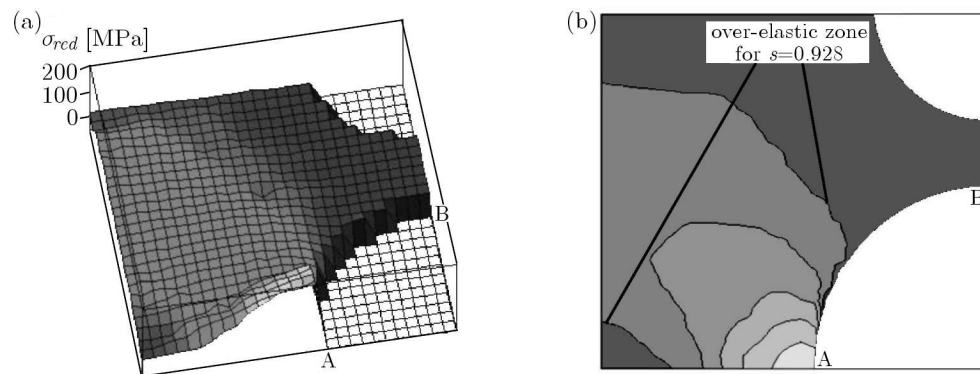


Fig. 8. Analyzed area of model IV at the loading level –  $s = 0.928$ : (a) reduced stress  $\sigma_{red}$  distribution, (b) range of over-elastic area

In many practical cases, we deal with the elements having a geometric and loading plane of symmetry. The determination of strain and stress components along the axis of symmetry is simpler in comparison with the solution of the full plane problem. Such analysis often allows estimating the maximum values of strains and stresses in the whole plastified area.

The distribution of strain and stress components in a partly plastified area along the  $x$  axis of symmetry (perpendicular to the stretching direction) is presented for model II (with slot) at the loading level  $s = 0.952$ , which corresponds to tensile stresses  $p = 87$  MPa.

For the strain separation, the simplified method of characteristics was used, which is presented in papers by Kapkowski and Kozłowska (1993), Kozłowska (1996). The values of stress components were calculated on the basis of the same 6-sectional model of the material characteristic.

The isochromatic pattern taken from the dark-field polariscope for model II is shown in Fig. 9a, and like previously, one quarter of the tested area was considered. The segment A-B means the part of the models axis of symmetry, where the values of strain and stress were calculated. The distribution of strain components  $\varepsilon_x$  and  $\varepsilon_y$  on the segment A-B is presented in Fig. 9b. On the same diagram, the strain distribution found using experimental Moiré method and from numerical (FEM) calculations are shown. These investigations were performed by the author (Kozłowska, 2008).

As it results from these diagrams, the  $\varepsilon_x$  and  $\varepsilon_y$  distribution on the  $x$  axis of symmetry obtained from the photoelastic coating method is approximated to this received from the Moiré method. The differences between both experimental methods are about 6-8%. A little bigger difference can be found when comparing experimental and FEM data, but even then it does not exceed 12%.

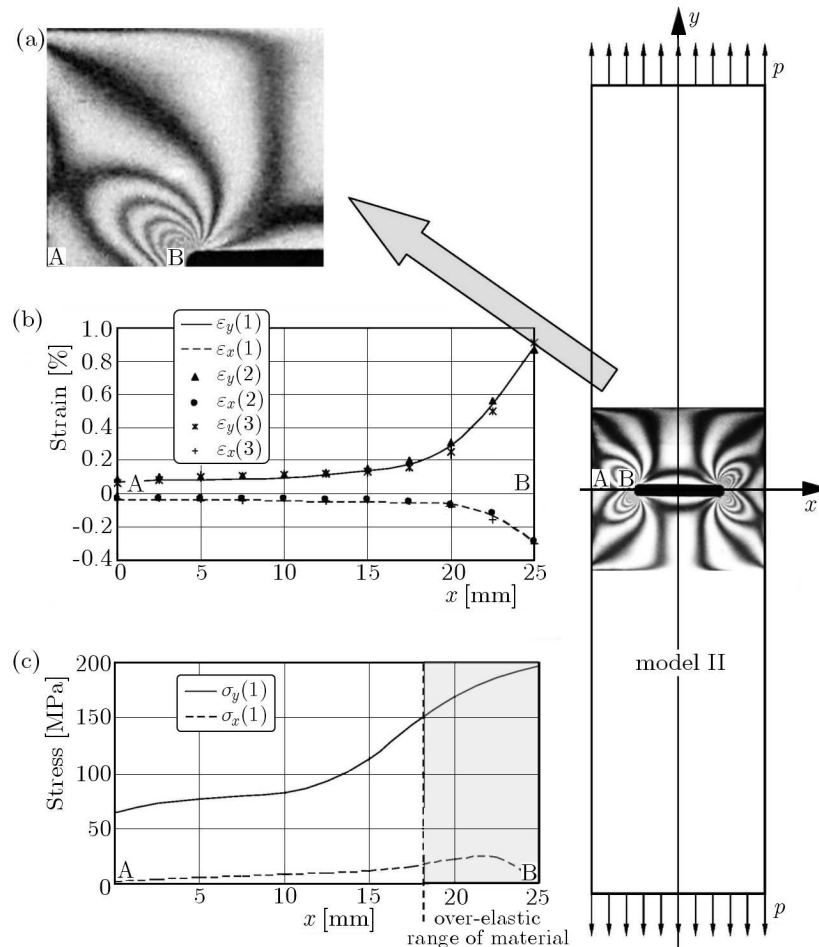


Fig. 9. Analyzed area of model II at loading level –  $s = 0.952$ : isochromatic pattern (a), strain  $\varepsilon_x$  and  $\varepsilon_y$  distribution (b), stress  $\sigma_x$  and  $\sigma_y$  distribution (c); on diagrams: (1) – photoelastic coating method, (2) – Moiré method, (3) – FEM calculations

The distribution of stress components  $\sigma_x$  and  $\sigma_y$  on the segment A-B is presented in Fig. 9c. On the diagram, the range of the plastic zone on the  $x$  axis of symmetry is marked.

## 5. Conclusions

Proper estimation of the strain and stress components in plastified zones of constructional elements is very important considering the safety of the whole construction.

In the paper, the author presents quantitative analysis of strains and stresses, which occur in stretched models of constructional elements weakened by holes of different shapes and groups of circular holes.

The experimental testing was carried out by the photoelastic coating method, and for further analysis pictures of the isochromatic pattern were only used.

For the strains separation and the values of stresses calculation, the 6-sectional model of material characteristics was accepted. Such a model (considering the number of segments) is quite sufficient for a proper representation of the experimental  $\sigma(\varepsilon)$  curve, what was confirmed by the smoothness of stress surfaces in the points, where the material is passing into the non-elastic state.

The obtained results showed that the applied method allows determination of strain and stressing distributions with a satisfactory accuracy. Results of the experimental analysis were compared with those obtained from the investigations carried out by the “in-plane” Moiré method and FEM calculations. The differences between the results obtained from the two experimental methods, which were based on different measurements (the photoelastic coating method – strain measurement, the Moiré method – displacement measurement) were about a few percent. The differences between experimental and FEM results do not exceed 12%.

The range of application of the method of photoelastic coating depends mostly on the thickness of the photoelastic layer (usually 1-3 mm) and material properties of the tested object. For the investigated duralumin elements a 2 mm thick layer was used, what enabled one to distinguish isochromatic lines corresponding to the maximum plastic strain of 0.9%. For the investigation of the elements by Moiré method, the 20 lines/mm grids were used, which allowed to determine maximum plastic strain of 1.5% (Kozłowska, 2008). Both experimental methods enable to measure or determine strain components with accuracy of  $\sim 0.01\%$ .

Among different experimental methods which may be applied to the analysis of elastic-plastic strain fields, the method of photoelastic coating is one of the best.

The greatest advantage of this method is the possibility of easy and prompt localization of the plastic zones which should be carefully controlled.

The advantage of the method is also the direct strain measurement. However, it must be noted that the obtained results depend on the material properties of the tested element, when for strain separation the method of characteristics is used.

On the basis of the obtained results, it can be concluded that the photoelastic coating method can be applied successfully to the strains and stresses analysis in two-dimensional elastic-plastic problems. It can be used, therefore, as an experimental tool for verification of engineering designs.

## References

1. DIAZ E.V., ARMAS A.E, KAUFMANN G.H., GALIZZI G.E., 2004, Fatigue damage accumulation around a notch using a digital image measurement system, *Experimental Mechanics*, **44**, 3, 241-246
2. FONTANARI V., BELLIN F., VISINTAINER M., ISCHIA G., 2006, Study of pressure sensitive plastic flow behaviour of gasket materials, *Experimental Mechanics*, **46**, 6, 313-323
3. FRANCK C., HONG S., MASKARINEC S.A., TIRRELL D.A., RAVICHANDRAN G., 2007, Three-dimensional full-field measurements of large deformations in soft materials using confocal microscopy and digital volume correlation, *Experimental Mechanics*, **47**, 3, 427-438
4. GUROVA T., TEODÓSIO J.R., REBELLO J.M.A., MONIN V., 1998, Model for the variation of the residual stress state during plastic deformation under uniaxial tension, *Journal of Strain Analysis*, **33**, 5, 367-372
5. HALDRUP K., NIELSEN S.F., WERT J.A., 2008, A general methodology for full-field plastic strain measurements using X-ray absorption tomography and internal markers, *Experimental Mechanics*, **48**, 2, 199-211
6. KAPKOWSKI J., KOZŁOWSKA B., 1993, Elastic-plastic strain analysis by photoelastic coating method, *Journal of Theoretical and Applied Mechanics*, **31**, 3, 493-512
7. KAPKOWSKI J., SŁOWIKOWSKA I., STUPNICKI J., 1987, *Badanie naprężeń metodą elastoptycznej warstwy powierzchniowej*, PWN, Warszawa
8. KELLEHER J., PRIME M.B., BUTTLE D., MUMMERY P.M., WEBSTER P.J., SHACKLETON J., WITHERS P.J., 2003, The measurement of residual stress in railway rails by diffraction and other methods, *Journal of Neutron Research*, **11**, 4, 187-193
9. KOZŁOWSKA B., 1996, *Zastosowanie metody elastoptycznej warstwy powierzchniowej do analizy stanów sprężysto-plastycznych*, Phd Thesis, Warszawa [no publication]

10. KOZŁOWSKA B., 2008, Strain and stress analysis in two-dimensional elastic-plastic state by Moiré method, *Transactions of FAMENA*, **XXXII**, 1, 19-26
11. LIVIERI P., NICOLETTO G., 2003, Elastoplastic strain concentration Factors in Finite Thickness plates, *Journal of Strain Analysis*, **38**, 1, 31-36
12. MILKE J. G., BEUTH J. L., BIERY N. E., 2000, Notch strengthening in titanium aluminides under monotonic loading, *Experimental Mechanics*, **40**, 4, 415-424
13. PADMANABHAN S., HUBNER J.P., KUMAR A.V., IFJU P.G., 2006, Load and boundary condition calibration using full-field strain measurement, *Experimental Mechanics*, **46**, 5, 569-578
14. PASTRAMA S.D., ILIESCU N., ATANASIU C., 2005, Photoelastic analysis for overdeterministic calculation of the stress intensity factor, *Proceedings of 22nd DANUBIA-ADRIA Symposium on Advances in Experimental Mechanics*, Parma 2005, 45-46
15. RASTY J., LE X., BAYDOGAN M., CÁRDENAS-GARCÍA J.F., 2007, Measurement of residual stresses in nuclear-grade zircaloy-4(R) tubes effect of heat treatment, *Experimental Mechanics*, **47**, 2, 185-199
16. SZCZEPIŃSKI W., 1964, Method of characteristics in computation of the experimental stress analysis, *Bulletin de l'Académie Polonaise des Sciences*, **XII**, 112
17. TIMOSHENKO S., GOODIER J.N., 1962, *Teoria sprężystości*, Wyd. Arkady, Warszawa
18. TONG W., 2004, Plastic surface strain mapping of bent sheets by image correlation, *Experimental Mechanics*, **44**, 5, 502-511
19. WUNG P., WALSH T., OURCHANE A., STEWART W., JIE M., 2001, Failure of spot welds under in-plane static loading, *Experimental Mechanics*, **41**, 1, 100-106
20. ZANDMAN F., REDNER S., DALLY J.W., 1977, *Photoelastic Coatings*, SESA Monograph 3, Westport

### Doświadczalna analiza odkształceń i naprężeń w dwuwymiarowych stanach sprężysto-plastycznych

#### Streszczenie

W pracy została przedstawiona ilościowa analiza odkształceń i naprężeń w obszarach sprężysto-plastycznych w płaskich modelach elementów konstrukcyjnych z koncentratorami naprężeń o różnych kształtach. Modele, wykonane z duraluminium, zostały obciążone równomiernie rozłożonymi na końcach naprężeniami rozciągającymi wywołującymi częściowe uplastycznienie materiału. Badania eksperymentalne zostały przeprowadzone przy pomocy metody elastoptycznej warstwy powierzchniowej. Do rozdzielania odkształceń zastosowano analityczną metodę charakterystyk wykorzystującą do obliczeń wyłącznie obraz izochrom. Składowe stanu odkształcenia i naprężenia w obszarach uplastycznionych zostały wyznaczone na podstawie wieloodcinkowego modelu krzywej dla materiału elementu. W pracy została przeprowadzona dyskusja otrzymanych wyników i ich porównanie z wynikami otrzymanymi metody mory i obliczeń numerycznych (MES).

*Manuscript received May 8, 2012; accepted for print July 6, 2012*